Examining the Madden-Julian Oscillation in Climate Models

MIDN 1/C Cameron Jackson[1], Prof. Bradford S. Barrett[1], and Assoc. Prof. Gina Henderson[1]
[1]Oceanography Dept., U.S. Naval Academy, Annapolis MD 21402

Introduction

Intraseasonal tropical climate variability has important implications for mid- and high-latitude climate. Recent studies have found modulation of a number of weather processes in the Northern Hemisphere, such as snow depth (Guan et al. 2012; Barrett et al. 2015; Li et al. 2016), sea ice concentration (Henderson et al. 2014), precipitation (Donald et al. 2006), atmospheric rivers (Higgins et al. 2000), and air temperature (Vecchi and Bond 2004; Seo et al. 2016; Zhou et al. 2016). In such studies, the leading mode of tropical intraseasonal variability, the Madden-Julian Oscillation (MJO), has tended to lag tropical convection by approximately 7 days. However, such consensus is still absent when considering the relationship and lag between the MJO and the Antarctic atmosphere. Flatau and Kim (2013) suggested a lag of 7-10 days between the Antarctic Oscillation (AAO) and the MJO, while Fauchereau et al. (2016) and Henderson et al. (2018) suggested important lags between MJO convection and extratropical circulation out to 20 days.

This study builds on previous work by **creating an index to detect the MJO signal** in datasets that measure or simulate zonal wind and outgoing longwave radiation**.** The goal is to use that signal to examine the MJO in climate models, including in Antarctica.

Tropical-Antarctic teleconnections

What is the MJO?

- A large-scale mode of atmospheric tropical variability
- Moves generally eastward around the equator on a time scale of 30-60 days.
- Most active in the eastern hemisphere (Indian Ocean to Western Pacific Ocean).

How is the MJO connected to Antarctica?

- The large-scale latent heat release of the MJO convection excited poleward-moving Rossby Waves
- Those Rossby waves modulate surface pressure and circulation, which then modulate ice (**Fig. 1**)

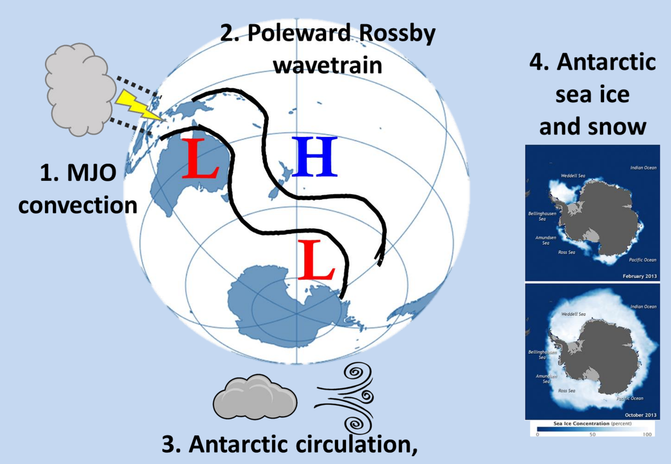

Figure 1: Schematic of the MJO's influence from the tropics to the extratropics

Methodology

In order to emulate the Wheeler Hendon RMM index for CMIP6 model output, we followed the framework set out in an NCL code example to construct a methodology to do the following:

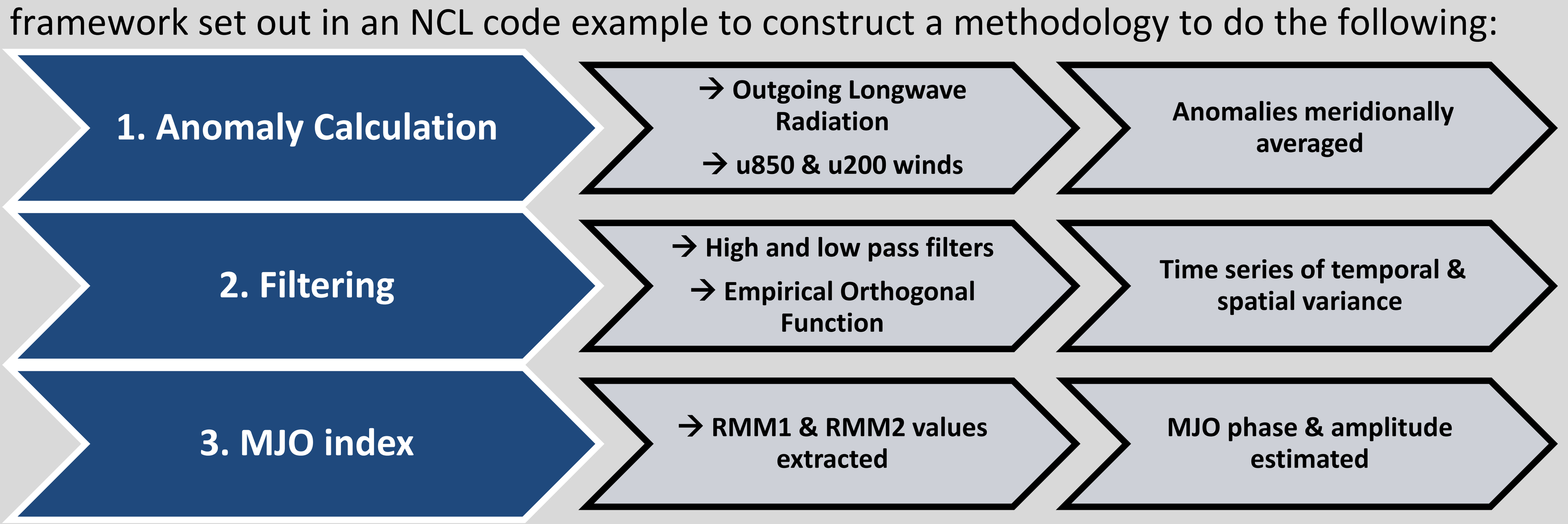

The resultant MJO metric that we calculate will hereafter be referred to as the Jackson MJO (JM) index.

Data and Methods

The analyses in this study were based on two publicly available datasets:

1. NOAA Earth System Research Laboratory - Physical Sciences Division (ESRL-PSD) reanalysis:
- Daily values of OLR
- Daily U-component of 200 and 850 hPa winds

The above three variables were analyzed with respect to time from January 1975 to December 2018, and geographically from latitudes 15°S to 15°N for all longitudes

- Index values calculated using data from January 1st, 1975 through December 31st, 2018 were used to construct the scatter plots in Result 1.

2. Real-time Multivariate MJO (RMM) Index (Wheeler and Hendon 2004; hereafter, WH04)
- RMM index includes eight phases, each one corresponding to a broad geographic location of the MJO's enhanced equatorial convective signal.

For this study, days when the RMM amplitude was greater than 1.0 were classified as "active".

- The RMM index has been calculated numerous times before- our purpose in calculating it again is to be able to replicate previous RMM indices and be able to apply it to climate model output

Results

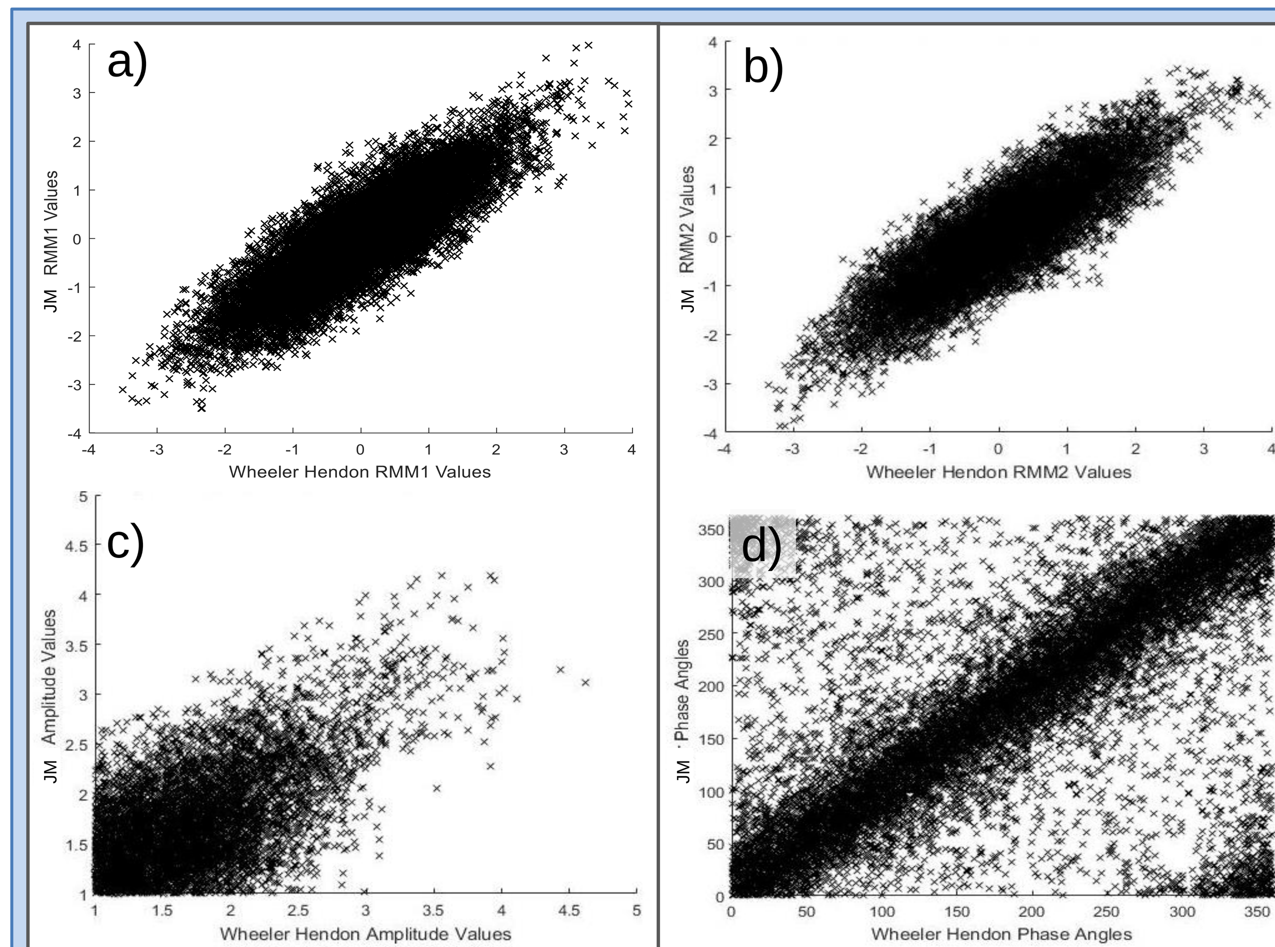

Figure 1: Scatter plots of the JM index values versus index values calculated by the Australian Bureau of Meteorology from 1st Jan 1975 to 31st Dec 2018, for a) RMM1, b) RMM2, c) Amplitude, and d) Phase Angle.

Result 1: Comparison with Wheeler-Hendon RMM

- Daily values of JM RMM1, RMM2, amplitude, and phase angle were compared with daily values of the Wheeler-Hendon (WH, 2004) MJO index calculated by the Australian Bureau of Meteorology (WH04).
- When comparing the JM and WH MJO indices:
  - The JM and WH RMM1 and RMM2 principal components were strongly linearly correlated, with correlation coefficients of 0.85 (Fig. 1a) and 0.86 (Fig. 1b).
  - The correlation coefficient for JM and WH amplitude was less than for RMM1 and RMM2 (0.72: Fig. 1c). One possible reason for this weaker correlation is because the correlation coefficient accounts for all days, not just active MJO days, so amplitude values < 1.0 are included in the coefficient and could result in a weaker linear correlation between JM and WM amplitudes.
  - The correlation coefficient for JM and WH phase angle was less than RMM1, RMM2, or amplitude (0.59: Fig. 1d).

Future Work:

- Indices for MJO from the CMIP6 data will be compared to WH and JM data in a similar manner as this comparison.
- Scatter plots will be used to visually determine the level of linear correlation between CMIP6 model indices and JM/WH indices, as well as correlation coefficients for each index.

Result 2: Phase-space Comparison

- Resulting JM indices were compared to the Australian Bureau of Meteorology (WH04) and NCL RMM1 and RMM2 for two time periods:
  - October 1st, 2018 to December 31st of 2018 (Fig. 2).
  - October 16th, 1996 to April 15th, 1997 (Fig. 3).
- In comparing our methodology to either the Australian Bureau of Meteorology or the NCL NCAR estimate, we seem to be capturing approximately the correct amplitude of MJO index (proximity from center of RMM diagram), however our phase estimate is slightly lagged.
- Confidence in the JM methodology comes from the similarity between the top figures, which originated from outside sources, and the bottom figures, which were produced by our MJO phase estimation.

Future Work:

- CMIP6 model data can be used to create phase space diagrams similar to those seen in figures 2 and 3.
- The process used to create the JM index can be duplicated with the use of CMIP6 data in order to create phase space diagrams and other products that can aid in the prediction of future MJO behavior and patterns.
- The replication of the process used to create the JM index is straightforward and allows for the use of a wide variety of model data to predict future MJO behavior and its tropical-Antarctic teleconnections.

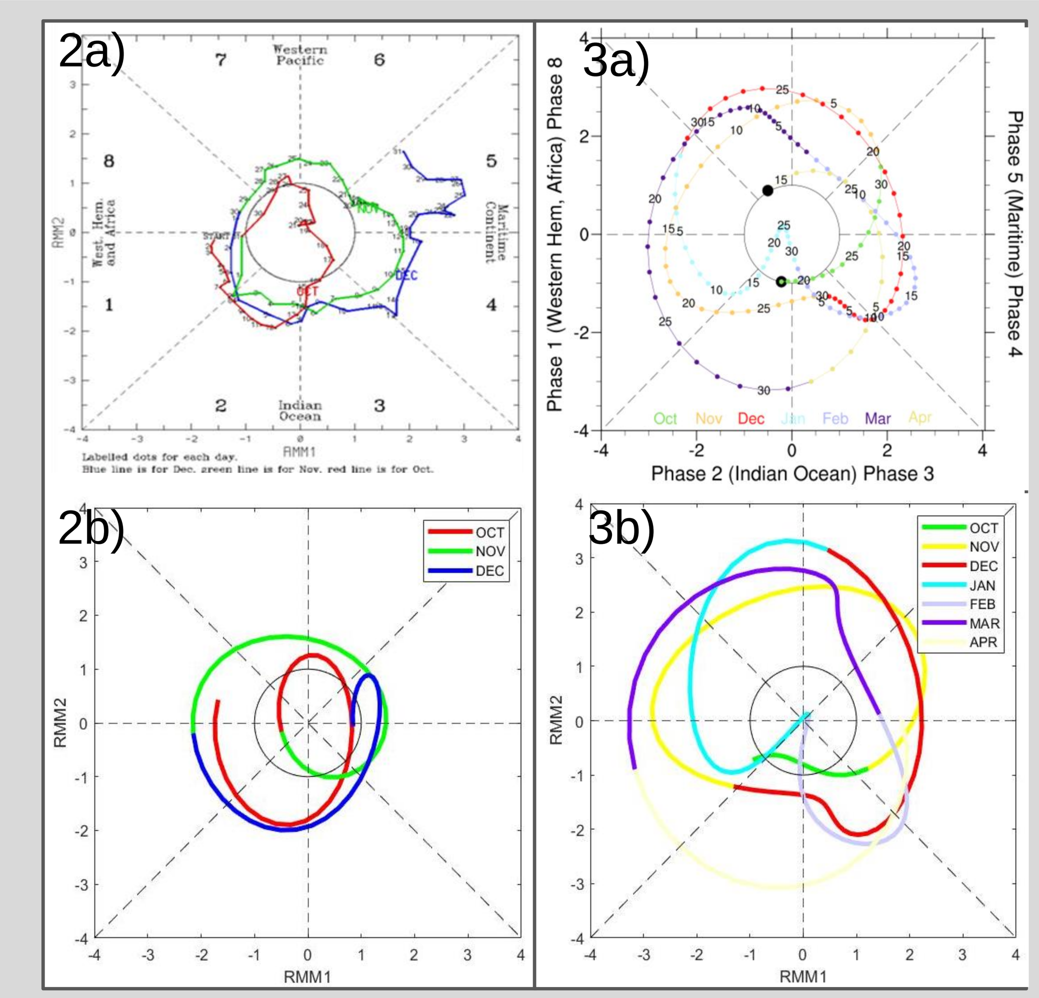

Figure 2: MJO phases from 1st Oct to 31st Dec 2018, from a) Australian Bureau of Meteorology WH04 (MJO), and b) JM phase estimate.

Figure 3: MJO phases from 16th Oct 1996 to 15th Apr 1997, from a) NCL NCAR (MJO CLIVAR), and b) JM phase estimate.

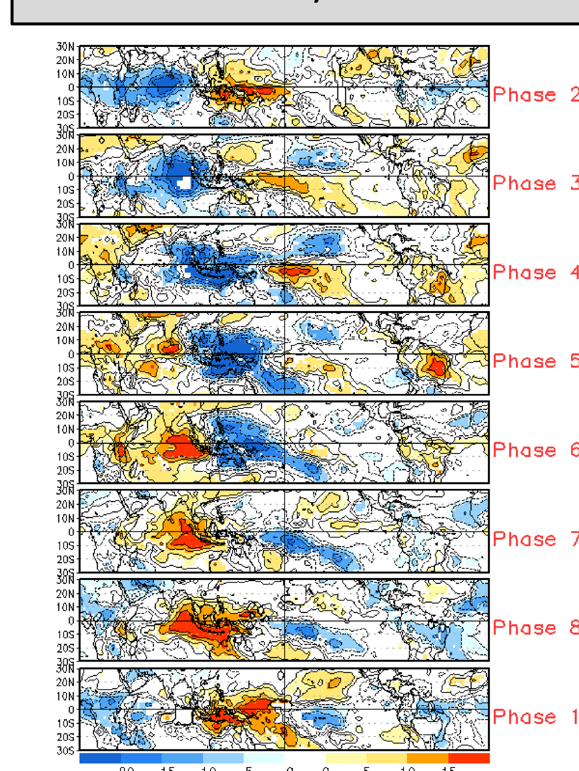

Figure 4: OLR global composite over all longitudes & latitudes from 30N to 30S, NOAA (Climate Prediction Center).

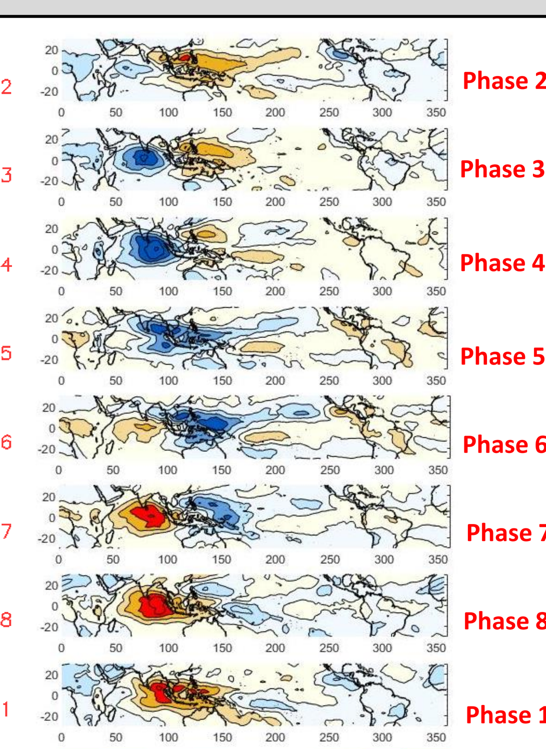

Figure 5: OLR global composite over all longitudes & latitudes from 30N to 30S, our spatial composite estimate.

Result 3: OLR spatial composites

- OLR spatial composites by MJO phase were plotted for Nov-Mar for both JM and WH04 methods:
  - OLR composite from the NOAA Climate Prediction Center (Fig. 4).
  - OLR composite from the JM spatial composite estimate (Fig. 5).
- In comparing the JM composites to those of the Climate Prediction Center, we seem to be capturing approximately the eastward propagation of an area of decreased OLR (blue coloration), which occurs to the east of an area of increased OLR (orange coloration) for all MJO phases. The strength of these primary areas of increased/decreased OLR are similar: in both composites, the area of increased OLR has a strength of 5 to 15 W m^{-2}, and the area of decreased OLR has a strength of -10 to -20 W m^{-2}.
- The accuracy of our methodology can be seen in the similarity between Figures 4 (from NOAA WH04) and 5 (from the JM methodology).

Future Work:

- CMIP6 OLR data could be used to create similar OLR spatial composites for future behavior of the MJO.

References

Barrett, B. S., G. R. Henderson, and J. S. Werling, 2015: The influence of MJO on the intraseasonal variability of Northern Hemisphere spring snow depth. *J. Climate*, **28**, 7250-7262.

Donald, A., H. Meinke, B. Power, A. H. N. de Maia, M. C. Wheeler, N. White, R. C. Stone, and J. Ribbe (2006), Near-global impact of the Madden-Julian oscillation on rainfall. *Geophys. Res. Lett*., **33**, L09704, doi:10.1029/2005GL025155.

Fauchereau, N. N., B.B. Pohl, and A.A. Lorrey, 2016: Extratropical impacts of the Madden–Julian Oscillation over New Zealand from a weather regime perspective. *J. Climate*, **29**, 2161–2175, doi: 10.1175/JCLI-D-15-0152.1.

Flatau M. and Y. J. Kim, 2013: Interaction between the MJO and polar circulations. J. Clim. 26: 3562–3574.

Guan, B., D. E. Waliser, N. P. Molotch, E. J. Fetzer, and P. J. Neiman, 2012: Does the Madden–Julian Oscillation influence wintertime atmospheric rivers and snowpack in the Sierra Nevada?. *Mon. Wea. Rev.,* **140**, 325–342, doi: 10.1175/MWR-D-11-00087.1.

Henderson, G. R., B. S. Barrett, and D. M. LaFleur, 2014: Arctic sea ice and the Madden-Julian Oscillation (MJO). *Climate Dyn*., **43**, 2185-2196. doi:10.1007/s00382-013-2043-y.

Higgins, R. W., J.-K. E. Schemm, W. Shi, and A. Leetmaa (2000), Extreme precipitation events in the Western United States related to tropical forcing, *J. Climate*, **13**, 793–820.

Li, W., W. Guo, P. Hsu, and Y. Xue, 2016: Influence of the Madden–Julian oscillation on Tibetan Plateau snow cover at the intraseasonal time-scale. *Scientific Reports*, *6*, 30456. http://doi.org/10.1038/srep30456.

Seo, K.-H., H. Lee, and D.W. Frierson, 2016: Unraveling the teleconnection mechanisms that induce wintertime temperature anomalies over the Northern Hemisphere continents in response to the MJO. *J. Atmos. Sci.,* **73**, 3557–3571, doi: 10.1175/JAS-D-16-0036.1.

Vecchi, G. A., and N. A. Bond (2004), The Madden-Julian Oscillation (MJO) and northern high latitude wintertime surface air temperatures. *Geophys. Res. Lett*., **31**, L04104, doi:10.1029/2003GL018645.

Zhou, Y., Y. Lu, B. Yang, J. Jiang, A. Huang, Y. Zhao, M. La, and Q. Yang, 2016: On the relationship between the Madden-Julian Oscillation and 2 m air temperature over central Asia in boreal winter. *J.Geophys. Res. Atmos.*, **121**, 13,250-13,272.

Acknowledgements

The authors gratefully acknowledge support from the NSF Office of Polar Programs (OPP), award no. 1821915.